PAPER Nr.: 49

FEASIBILITY STUDY OF A FIRE FIGHTING HELICOPTER FOR HIGH BUILDINGS

BY

S.SAITO, Y.OKUNO, M.HARADA, K.FUNABIKI

NATIONAL AEROSPACE LABORATORY
TOKYO, JAPAN

AND

S.AKAMATSU

THE UNIVERSITY OF TOKYO
TOKYO, JAPAN

TWENTIETH EUROPEAN ROTORCRAFT FORUM
OCTOBER 4 - 7, 1994 AMSTERDAM

Printed by the Technical Highschool Haarlem

FEASIBILITY STUDY OF A FIRE FIGHTING HELICOPTER FOR HIGH BUILDINGS

Shigeru SAITO, Yoshinori OKUNO, Masashi HARADA, Kohei FUNABIKI
National Aerospace Laboratory
6-13-1, Osawa, Mitaka, Tokyo, Japan 181
and
Shigeki AKAMATSU
Faculty of Aeronautics and Astronautics, the University of Tokyo
7-3-1, Hongo, Bunkyo-ku, Tokyo, Japan 113

Abstract

A helicopter is now being considered as a candidate to extinguish a fire of high buildings. This paper investigates the feasibility of the fire fighting helicopter, which has the capability of carrying one ton water inside the cabin, hovering in the turbulent wind nearby a building, and hitting the water on the target window by using a water ejection system. The following three methods were used for this study: (1) linearized analysis considering the effects of the turbulence, automatic control system, and the weight change and reaction force during the water ejection, (2) flight simulation tests considering the collaboration of the pilot and the ejection boom operator, and (3) flight tests including hovering flights nearby a real high building. As the results of these investigations, it was shown that the assumed fire fighting helicopter based on an existing large size helicopter has an enough capability to make hovering at a distance of 20 m from the building wall up to a wind speed of 7 m/s and can hit nearly 80% of the ejected water on the target window.

1. INTRODUCTION

In case of fire at a high building in a metropolitan city such as Tokyo, the fire fighting may be difficult by the fire engines alone. A helicopter is therefore considered to extinguish the burning building because of its capability of hovering flight. A large helicopter of 8 to 10 ton class is assumed as a candidate of the fire fighting helicopter owing to its high payload capability and wide safety margin. Figure 1 shows a design concept of this fire fighting helicopter. This helicopter carries one ton water inside the cabin and has a water pressurizing system to eject the water. Two retractable and controllable ejection booms are installed on both sides of the helicopter, the length of which is longer than the rotor radius to avoid the effect of the rotor downwash.

The outline of the fire fighting operation is as follows:

Phase I: The helicopter approaches the burning building. The operation will be canceled if the wind is too strong to operate safely.

Phase II: The helicopter makes hovering at a distance of 20 m from the building (this distance is determined by a trade-off between safety margin and efficiency of the fire fighting operation). The heading of the helicopter is kept parallel to the building wall so that the helicopter can easily fly away in case of emergency. The fire fighting operation is started by the ejection boom operator in collaboration with the pilot. The operation time is nearly 100 seconds.

Phase III: After finishing the fire fighting operation or in case of emergency, the helicopter leaves the building. The helicopter returns to a base, supplied, and fights again.

The major problems for a safe and efficient fire fighting operation are the effects of wind turbulence and water ejection on the helicopter dynamics and the human factors in position keeping and ejection boom control. Since the complex and unsteady turbulence around high buildings affects the helicopter dynamics, the decision criteria to cancel the operation must be determined by estimating this effect on the accuracy of position keeping during approach, hover and leaving. It also affects the accuracy of the water beam targeting. Therefore collaboration between the ejection boom operator and the pilot is an important factor for a safe and efficient fire fighting operation.

There are many investigations about an effect of the turbulence on the rotor aerodynamics and/or the flight dynamics [1, 2, 3] but less investigations have been made about the structure of the turbulence around high buildings in the aeronautical field. There are however many investigations in the architectural field [4, 5]. Figure 2 shows typical flows around various buildings [4]. The flow is very complicated and so difficult to predict because vortices exist in the flow past through the corner of a building. In this study, the data of wind velocities were used, which were measured for both wind tunnel models and a real building.

This paper describes a theoretical method to investigate the dynamic response of a helicopter in the turbulence around a building, simulation tests performed to investigate the operational limitations of the fire fighting helicopter, flight tests to investigate the dynamic characteristics of a helicopter during hover (flight test A), and flight tests to validate the feasibility of the fire fighting operation (flight test B). As the results of these investigations, hovering ability nearby a building and fire fighting ability, which is estimated by the water hitting ratio to a window of burning building, will be discussed. The Aerospatial 332L1 Super Puma helicopter, which is 8 ton in weight and 14 m in the rotor diameter, is adopted as an assumed fire fighting helicopter.

2. THEORETICAL ANALYSIS

Numerical simulations using the linearized equations of motion were performed to estimate the accuracy of hovering nearby a building and fire fighting operation. Figure 3 shows the block diagram of this analysis. The aerodynamic derivatives were fundamentally derived from a theoretical analysis with non-uniformed induced velocity, although they were identified from flight test data later. The effect of the turbulence around a building was estimated in a statistical manner because the turbulence is essentially random. This simulation also includes the effects of the reaction force of the ejected water, inertial force caused by the rapid and continuous weight reduction, and the automatic control system installed (and will be installed) on board. The ejection boom is assumed to be fixed and so the reaction force caused by the motion of the ejection boom are not taken into account.

Basic equations

The basic linearized equations of motion of a helicopter are given as follows:

$$\mathbf{m}\dot{\mathbf{x}} = \mathbf{A}\mathbf{x} + \mathbf{B}\mathbf{u} + \mathbf{G}\mathbf{g} \tag{1}$$

where

$$\begin{aligned}
\mathbf{m} &= (m, m, I_{yy}, 1, m, I_{xx}, 1, I_{zz}, 1) \\
\mathbf{x} &= (u, w, q, \Theta, v, p, \Phi, r, \Psi)^T \\
\mathbf{u} &= (\theta_0, \theta_S, \theta_C, \theta_T)^T \\
\mathbf{g} &= (u_g, w_g, v_g)^T
\end{aligned}$$

$$
\mathbf{A} = \begin{bmatrix}
X_u & X_w & X_q - mw_0 & X_\Theta & X_v & X_p & X_\Phi & X_r + mv_0 & 0 \\
Z_u & Z_w & Z_q + mu_0 & Z_\Theta & Z_v & Z_p - mv_0 & Z_\Phi & Z_r & 0 \\
M_u & M_w & M_q & 0 & M_v & M_p & 0 & M_r & 0 \\
0 & 0 & g\cos\Phi_0 & 0 & 0 & 0 & 0 & -g\sin\Phi_0 & 0 \\
Y_u & Y_w & Y_q & Y_\Theta & Y_v & Y_p + mw_0 & Y_\Phi & Y_r - mu_0 & 0 \\
L_u & L_w & L_q & 0 & L_v & L_p & 0 & L_r & 0 \\
0 & 0 & g\sin\Phi_0\tan\Theta_0 & 0 & 0 & 1 & 0 & g\cos\Phi_0\tan\Theta_0 & 0 \\
N_u & N_w & N_q & 0 & N_v & N_p & 0 & N_r & 0 \\
0 & 0 & g\sin\Phi_0\sec\Theta_0 & 0 & 0 & 0 & 0 & g\cos\Phi_0\sec\Theta_0 & 0
\end{bmatrix}
$$

$$
\mathbf{B} = \begin{bmatrix}
X_{\theta_0} & X_{\theta_s} & X_{\theta_c} & X_{\theta_T} \\
Z_{\theta_0} & Z_{\theta_s} & Z_{\theta_c} & Z_{\theta_T} \\
M_{\theta_0} & M_{\theta_s} & M_{\theta_c} & M_{\theta_T} \\
0 & 0 & 0 & 0 \\
Y_{\theta_0} & Y_{\theta_s} & Y_{\theta_c} & Y_{\theta_T} \\
L_{\theta_0} & L_{\theta_s} & L_{\theta_c} & L_{\theta_T} \\
0 & 0 & 0 & 0 \\
N_{\theta_0} & N_{\theta_s} & N_{\theta_c} & N_{\theta_T} \\
0 & 0 & 0 & 0
\end{bmatrix}, \quad
\mathbf{G} = -\begin{bmatrix}
X_u & X_w & X_v \\
Z_u & Z_w & Z_v \\
M_u & M_w & M_v \\
0 & 0 & 0 \\
Y_u & Y_w & Y_v \\
L_u & L_w & L_v \\
0 & 0 & 0 \\
N_u & N_w & N_v \\
0 & 0 & 0
\end{bmatrix}
$$

where the subscript 0 denotes the trimmed values.

Effect of water ejection and weight change

During the fire fighting operation, the weight of the helicopter decreases rapidly and the helicopter also receives the reaction force from the ejected water. As for the assumed fire fighting helicopter, water of about one ton is ejected at a flow rate of 10 kg/s from the ejection boom, which is 8 m long and has a nozzle of 16 mm diameter. As a result, the reaction force due to the water ejection was estimated as 40 kgf.

The governing equations were extended to include these effects of weight change and reaction force as follows:

$$
\mathbf{m}\dot{\mathbf{x}} = (\mathbf{A} - \mathbf{C})\mathbf{x} + \mathbf{B}\mathbf{u} + \mathbf{G}\mathbf{g} + \mathbf{F} + \mathbf{E} \tag{2}
$$

where $\mathbf{m}$ changes with the elapsed time, $\mathbf{C}$ is the inertial force for momentum conservation, $\mathbf{F}$ is the reaction forces and moments, and $\mathbf{E}$ is the virtual buoyancy caused by the weight reduction, i.e.,

$$
\mathbf{C} = diag(\frac{dm}{dt}, \frac{dm}{dt}, 0, 0, \frac{dm}{dt}, 0, 0, 0, 0)^T \tag{3}
$$

$$
\mathbf{E} = ((m_0 - m)g\sin\Theta_0, -(m_0 - m)g\cos\Phi_0\cos\Theta_0, 0, 0, -(m_0 - m)g\sin\Phi_0 cos\Theta_0, 0, 0, 0, 0)^T \tag{4}
$$

Although the aerodynamic derivatives also change with the weight reduction, this effect is neglected here.

Control systems

The control systems are divided into two parts; one is the stability system already installed on the assumed fire fighting helicopter, Super Puma, and the other is due to the pilot or the assumed position keeping control system.

The stability system installed on the Super Puma consists of the stability augmented system (SAS) and automatic stability equipment (ASE), which have the following feedback system respectively:

$$
\text{SAS}: \begin{cases} \theta_s = -K_{d_s}\dot{\Theta} \\ \theta_c = -K_{d_c}\dot{\Phi} \\ \theta_T = +K_{d_t}\dot{\Psi} \end{cases}, \quad
\text{ASE}: \begin{cases} \theta_s = -K_{d_s}\dot{\Theta} - K_{p_s}(\Theta - \Theta_{ref}) \\ \theta_c = -K_{d_c}\dot{\Phi} - K_{p_c}(\Phi - \Phi_{ref}) \\ \theta_T = +K_{d_t}\dot{\Psi} + K_{p_t}(\Psi - \Psi_{ref}) \end{cases} \tag{5}
$$

where K_{d_s}, K_{d_c}, K_{d_t}, K_{p_s}, K_{p_c}, K_{p_t} are the feedback gains of the real helicopter.

In this study, it is assumed that the ASE is always engaged, and in addition, three automatic control systems for position keeping were considered as follows: the first (control A) is a simple system simulating a pilot's control, in which the deviations from the prescribed position and velocities were fed back to the control inputs, the second (control B) is an optimized control law to maximize the water hitting ratio, which is tuned up not only in its gains but also in its rule to include feedback of the helicopter's attitude, and the third (control C) is a realistic control law, in which a system time delay of 0.2 sec is included in the control B.

Turbulence models

The turbulence models used in this study were based on the power spectrum of the experimental data, which were measured around a real building. Two measuring points were selected as shown in figure 4. One is located at the windward (point A), and the other is at the leeward (point C). Figure 5 show the power spectral densities of the measured wind velocities. A constant value of $D/U_0 = 7$ is assumed, where D is the width of the building and U_0 is the uniform wind speed. The wind at point A has a higher power spectrum in the low frequency region, while the wind at point C has a higher power spectrum in the high frequency region, due to the vortices generated at the corner of the building.

These measured wind velocities were simulated using white noise and filters. The typical filters for a uniform wind speed of 10 m/s at leeward side are given as follows:

$$u_g \;:\; 6 + \frac{3}{1 + s/1.8} z_1 \tag{6}$$

$$v_g \;:\; 8 + \frac{4}{1 + s/1.6} z_2 \tag{7}$$

$$w_g \;:\; 0 + \frac{2}{1 + s/2.0} z_3 \tag{8}$$

where z_i is a white noise.

Note that the scale of the turbulence is assumed to be larger than that of the helicopter rotor and accordingly the angular velocities of the turbulence are not taken into account.

Numerical simulation and analysis

Numerical simulations of the fire fighting operation were carried out considering the following parameters: (1) the strength of the uniform flow, i.e., mean wind speed, (2) relative position between the helicopter and the building (i.e., leeward or windward), which affects the power spectrum of the turbulence, and (3) kind of the control law. Hundreds of calculations were run for a set of these parameters, with the seed of the white noise, which was used to generate the turbulence, varying for each calculation. Each simulation was for 60 seconds in real time. The results of these simulations were averaged in a statistical manner.

The analyzed characteristics are (1) fluctuation of the flight path, which indicates the accuracy of position keeping, and (2) water hitting ratio, i.e., the ratio of the water amount which hit on the target window (assumed as 2 m $\times$ 2 m) to the whole ejected, which indicates the efficiency of the fire fighting operation.

3. SIMULATION TESTS

Simulation tests were conducted by using a flight simulator of the National Aerospace Laboratory in order to investigate the operational limitations of the fire fighting helicopter, i.e., the maximum wind speed at which a safe and efficient fire fighting operation can be performed.

Besides the cockpit of the flight simulator, an operator seat for the ejection boom control was set up (figure 6), at which the operator controls the lateral and vertical angles of the ejection boom by using a joy-stick type controller. The controllable ranges of the ejection boom are assumed as 90 ± 10 degrees in the lateral direction (measured from nose) and 7.5 ± 7.5 degrees

in the vertical direction (measured from horizon). The maximum moving rate is limited to be 3 deg/s, with a time constant of 0.3 sec being introduced to simulate the actuator delay.

On the visual screens of both the cockpit and the ejection boom operator seat, the targeted point was indicated by a red marker assuming a laser beam fixed on the ejection boom. The water hitting point was also indicated by a blue marker, although water beam itself was not drawn. The wind turbulence model around the building is same as Eqs.(6-8). So far, the effect of wind on the water beam is not taken into consideration. [1]

The pilot task was to keep the prescribed position and attitude (parallel to the building wall at a 20 m distance) or to hit the water on a target window (assumed as 2 m $\times$ 2 m) by controlling the helicopter's position and attitude.

4. FLIGHT TESTS

Flight test A

The flight tests to investigate the dynamic characteristics of the assumed fire fighting helicopter, Super Puma, during hover were performed in calm air at 150 feet above the ground (figure 7 (a)). The pilot inputted some scheduled controls such as sinusoidal, step, and impulse in the lateral/longitudinal stick, collective lever, and pedal. The following data were recorded: control inputs measured by the position transducers, accelerations, attitude and angular velocities measured by the IRU (Inertial Reference Unit). These data were used to identify the aerodynamic derivatives.

Flight test B

The flight tests to investigate the feasibility of the fire fighting operation were conducted nearby a building (figure 7 (b)) in a medium wind condition (the mean wind speed measured on the top of the building roof was 5.4 m/s). To simulate the water ejection, a search light was used to aim the target window (the search light was fixed on the left side of the helicopter). The pilot task was to control the helicopter to make the search light hit on the target window (at the 14th floor, nearly 50 m height above the ground) or to keep the prescribed position, i.e., 20 m distance from the target window without the search light. The data recorded were same as flight test A and, therefore, the trace of the search light hitting point was reconstructed using the position and attitude data measured by the IRU.

5. RESULTS AND DISCUSSIONS

Theoretical analysis

Figures 8(a)$\sim$9(b) show the ranges of the fluctuation in the circumferential direction (which means the averaged distance of drift) and the longitudinal direction (which means the average distance toward the building wall) for a mean wind speed of 7 m/s (this is thought to be a medium wind condition). The position keeping control system (control A) were engaged in these cases. The range of the movement may reach 2 m in the circumferential direction and 1 m in the longitudinal direction at the point A (windward) as can be seen from figure 8, while it is within 1.5 m and 0.75 m in each direction at the point C (leeward) as shown in figure 9. As a result, the assumed clearance of 20 m between the helicopter and the building wall was found to be adequate for a safe hovering flight. In addition, it is shown that the helicopter is more stable in the leeward of the building, because the turbulence in the leeward has a higher power spectrum in high frequency region, which has less effect on the helicopter dynamics. Note that this conclusion is drawn from a comparison of only two points of A and C. The turbulence around the corner of the building may have a more significant effect on the helicopter dynamics because of its complex and unsteady structure.

[1] Ground tests of the water pumping system are now being conducted by the Tokyo Fire Department and, therefore, our future work will include wind effect on the direction variation and scattering of the water beam.

Figure 10 shows the water hitting ratio, where it can be seen that less than 50 % of the ejected water can be hit on the target window at a mean wind speed of 7 m/s. Therefore, it was concluded that the efficient fire fighting operation can not be performed by the pilot alone, and some supporting equipment such as the ejection boom control system is necessary. It is also shown that the effect of the hovering point, i.e., whether at the windward or the leeward, has little effect on the hitting ratio.

Figure 11 compares the calculated results for three position keeping control laws along with the simulator test results. The simulator test results showed better performance than the first estimation using the position keeping control law which simulates a pilot's control (control A). A possibility is also shown to improve the hitting ratio when the assumed automatic position keeping system (control C) is installed on board. The results using the control B show the theoretical maximum of the fire fighting ability.

Simulation tests

Figure 12 compares the trace of the hitting point during one minute between the simulation and flight test results. Figure 12 (a) shows the water hitting point during the simulation test for the mean wind speed of 4 m/s, in which the pilot alone controlled the hitting point, i.e., the ejection boom was fixed; whereas figure 12 (b) shows the trace of the search light hitting point during the flight test B. Note that the hitting ratio is almost same between these two results, however, some differences are observed in their scattering patterns. Since the turbulence model adopted in the simulation test was based on a white noise, the simulated scattering pattern is also random. On the contrary, the flight test result seems to be sometimes affected by sudden and unexpected turbulence. This leads to the necessity for developing more real turbulence model around high buildings. [2]

Figure 13 shows the maximum and root mean square (rms) of the hitting error as a function of mean wind speed. The simulation test results (in which the ejection boom is fixed) show that both maximum and rms are almost linear to the wind speed. In comparison with the flight test result, the simulation test results show lower performance (i.e., large scattering), mainly because the flight simulator has less perspective owing to the limitation of the visual system and also did not have motion cues.

Figure 14 compares the hitting ratios among three combinations of the tasks of the pilot and the ejection boom operator. The rectangular symbols show the results when the pilot controlled the helicopter to hit the water on the target window, whereas the circular symbols show the results when the pilot was concentrated on keeping the initial position and attitude without attention to the hitting point. On the other hand, the solid symbols mean that the ejection boom was controlled by the operator (figure 15 exemplifies the time histories when controlling the ejection boom), although it was fixed in the open symbol cases. It is shown that when both the pilot and the ejection boom operator control the hitting point, nearly 90 % of the water can be hit on the target window up to a mean wind speed of 7 m/s. This performance seems to be enough for the fire fighting helicopter since in Tokyo only 5 % days through a year have a mean wind speed over 7 m/s. As the results of the simulation tests, the following conclusions are drawn:

1. When wind is calm (up to 4 m/s), efficient fire fighting operation can be performed by either the pilot or the ejection boom operator alone.

2. When wind is medium (up to 7 m/s), collaboration between the pilot and the ejection boom operator is necessary for a safe and efficient fire fighting operation.

3. When wind is heavy (up to 10 m/s), the hitting point sometimes falls wide of the target window and so on-off control of the pumping system is necessary for efficient use of the water.

[2] Our future simulation tests are planned to use the wind velocity time histories recorded at a real building.

4. Even when the pilot controls the hitting point in collaboration with the ejection boom operator, the increase in his workload is not so much as compared with that when concentrated on keeping the position and attitude.

5. The effect of the reaction force and weight change during water ejection can be easily controlled by the pilot.

Flight test A

The data measured during flight test A were used to identify the aerodynamic derivatives. Since a helicopter is always affected by turbulence even when flight tests are conducted in a calm wind condition at early morning, its effect must be considered in the trimmed condition. Therefore the initial values of the state variables must be included in the identification problem. The basic equations were rewritten into the following form:

$$m\dot{x} = m\dot{x}_0 + Ax + Bu \tag{9}$$

Table 1 shows the results of the identified derivatives by using the Least-Squares Estimation [6, 7]. Figure 16 compares the time histories of the flight test result with the reconstructed result using the identified derivatives. It can be seen that a good agreement is obtained between the flight test and reconstructed results.

Figure 17 shows the water hitting ratio as a function of the mean wind speed. In this figure, the theoretical results using the identified derivatives, the simulation test results (in which the ejection boom was fixed), and a result of the flight test B were compared to each other. Although the theoretical and simulation test results show good correlation, the result of the flight test B shows better performance than these results. It can be seen that the fire fighting helicopter has the capability of hitting more than 80 % of the ejected water on the target window in a calm wind condition up to 4 m/s without controlling the ejection boom.

Flight test B

In addition to the hitting ratio of the search light on the target window as mentioned above, the following results were also drawn from the pilot's comments during the flight test B:

1. Although the mean wind speed measured on the top of the building roof was 5.4 m/s, the pilot did not report any heavy turbulence during hover on the leeward of the building. The required pilot skill level was same as that of hovering on the roof top. On the other hand, medium turbulence was reported during hover around the corner of the building.

2. It was found to be difficult for the pilot to keep precisely the prescribed distance (20 m) from the building wall. The resultant distance varied from 16 m to 30 m. This necessitates the fire fighting helicopter to be installed with a distance indicator on board.

3. It was also difficult to keep a precise yaw attitude parallel to the building wall. The pilot had to refer to the heading indicator.

4. Since the pilot's view point was concentrated on outside the cabin, it was found to be very effective that the co-pilot calls the distance and heading to the pilot.

6. CONCLUSIONS

The feasibility of a fire fighting helicopter has been studied. First, the dynamic response of a helicopter in turbulence around a building was estimated using the linearized equations of motion in the statistical manner. The aerodynamic derivatives were theoretically estimated at first, and then identified from the flight test results. Second, the operational limitations of the fire fighting helicopter were investigated using the flight simulator. Third, the hovering capability nearby a building was validated by flight tests.

The results from these three methods showed reasonable correlation to each other. It was concluded that the assumed fire fighting helicopter based on an existing large size helicopter has an enough capability to perform a safe and efficient fire fighting operation in the medium wind condition up to 7 m/s.

In this paper, the problems at phase I (approach) and III (leaving) are not still investigated. Pilots indicated the importance of the flight procedure and operation manual. More detailed flight tests, simulation tests and analysis are necessary for these studies. These will be our future work.

ACKNOWLEDGMENTS

This research work has been conducted under the cooperation between National Aerospace Laboratory and Tokyo Fire Department. The authors would like to appreciate for their kind cooperation and usage of their helicopter. The authors also would like to express our thanks to the Shimizu Cooperation for their presentation of the data of turbulence around a building.

References

[1] G. H. Gaonkar and K. H. Hohenemser, An Advanced Stochastic Model for Threshold Crossing Studies of Rotor Blade Vibrations. AIAA J., Vol.10, No.8, pp.1100-1101, Aug. 1972.

[2] N. D. Ham, P. H. Bauer, T.H. Lawrence and M. Yasue, A Study of Gust and Control Response of Model Rotor-Propellers in a wind airstream. NASA CR-137756, Aug. 1975.

[3] A. Azuma and S. Saito, Study of Rotor Gust Response by Means of the Local Momentum theory, Journal of the American Helicopter Society, Vol.27, No.1, pp.58-72, January 1982.

[4] I. Kamei, Wind around buildings-Trend, Analysis and Counterplan, Journal of the Technology of Architecture, in Japanese, No.281, January 1975.

[5] B.E. Lee, The effect of turbulence on the surface pressure field of a square prism, Journal of the Fluid Mechanics, Vol.69, Part2, pp.263-282, 1975.

[6] V. Klein, Identification Evaluation Methods, AGARD-LS104, 1979.

[7] A. Tan, M. Komoda, A. Azuma, S. Saito, Y. Okuno, Theoretical and Experimental Studies on System Identification of Helicopter Dynamics, 20th European Rotorcraft Forum, October, 1994.

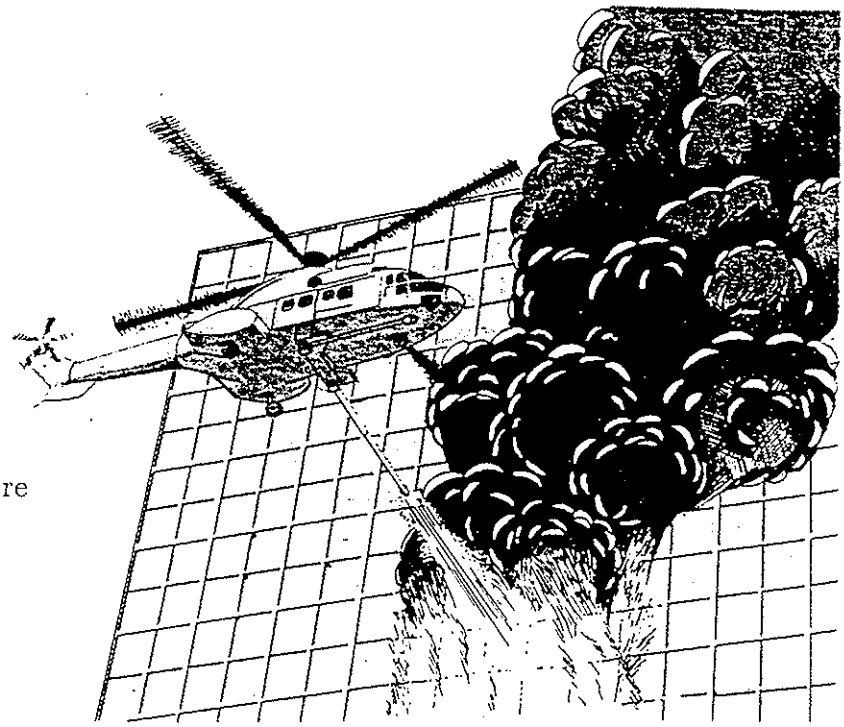

Figure 1 Schematic view of a fire fighting helicopter.

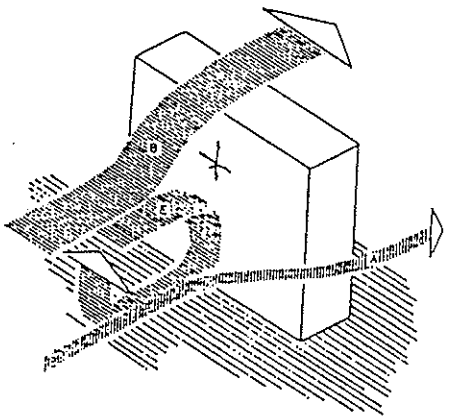

(a) Flow pattern around a wide building. (In the windward)

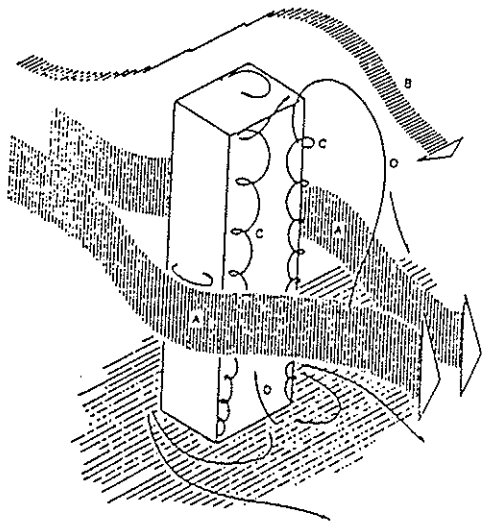

(c) Flow pattern around a high building. (In the leeward)

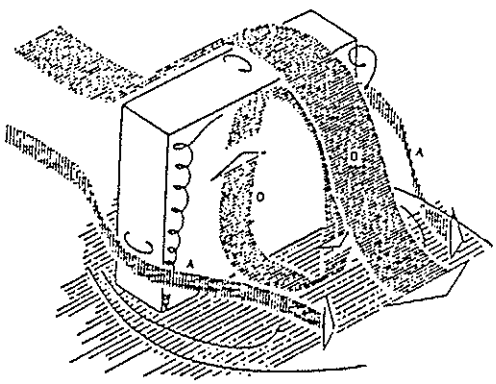

(b) Flow pattern around a wide building. (In the leeward)

Figure 2 Typical flow of wind around a building [4].

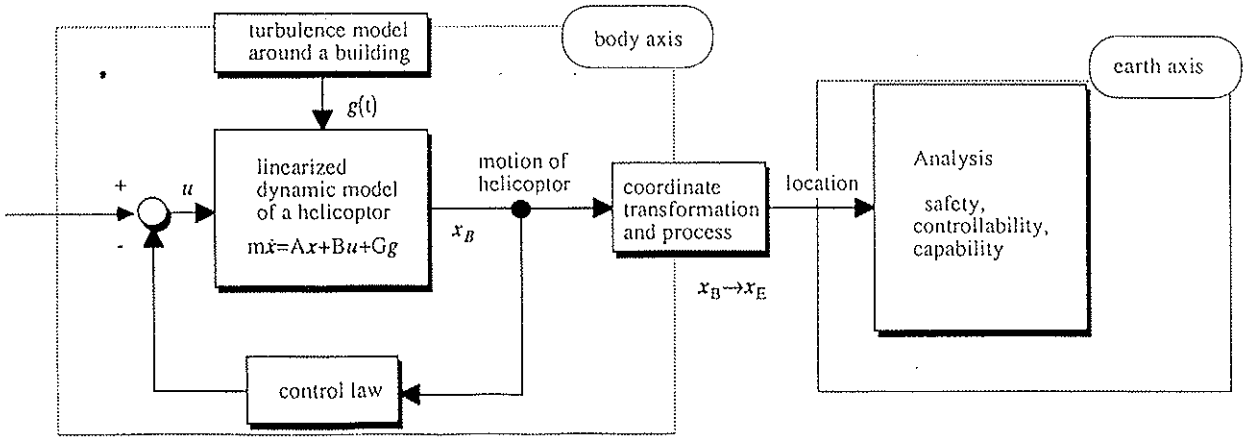

Figure 3 Block diagram for theoretical analysis.

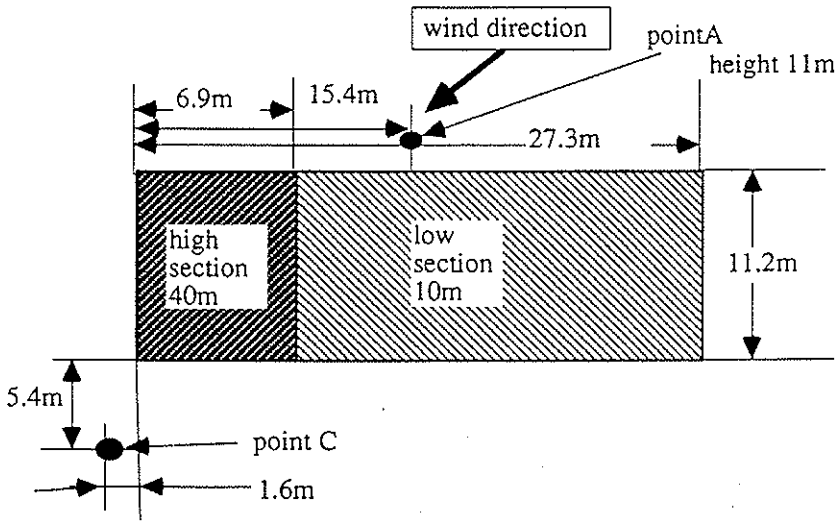

Figure 4 Measuring points of wind around a building.

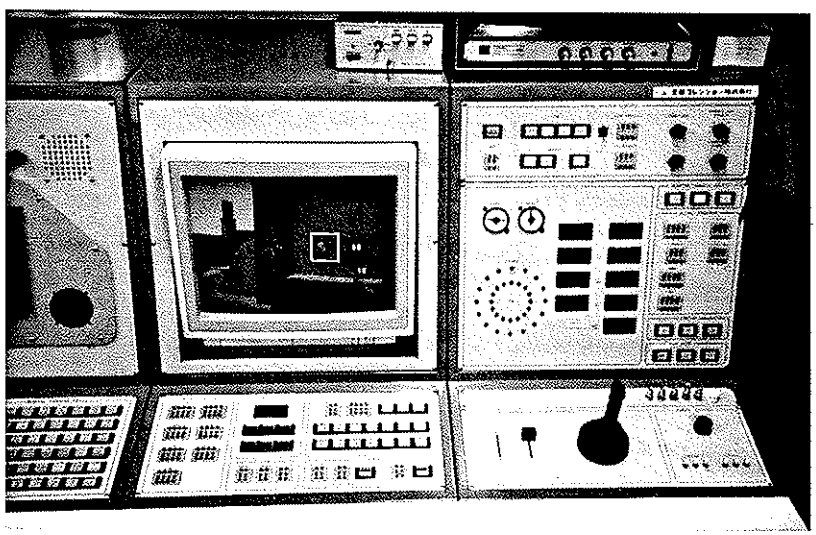

Figure 6 The control desk for the boom operator in the simulation test.

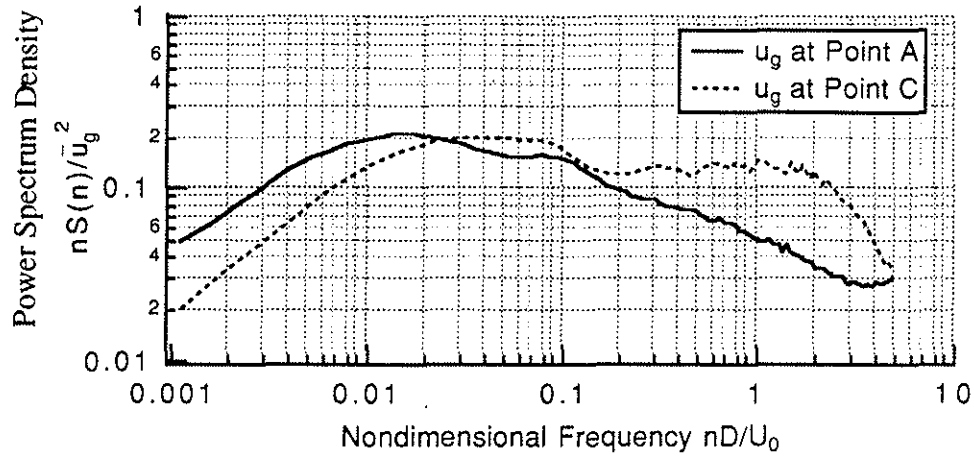

(1) $\mathbf{u}_g$

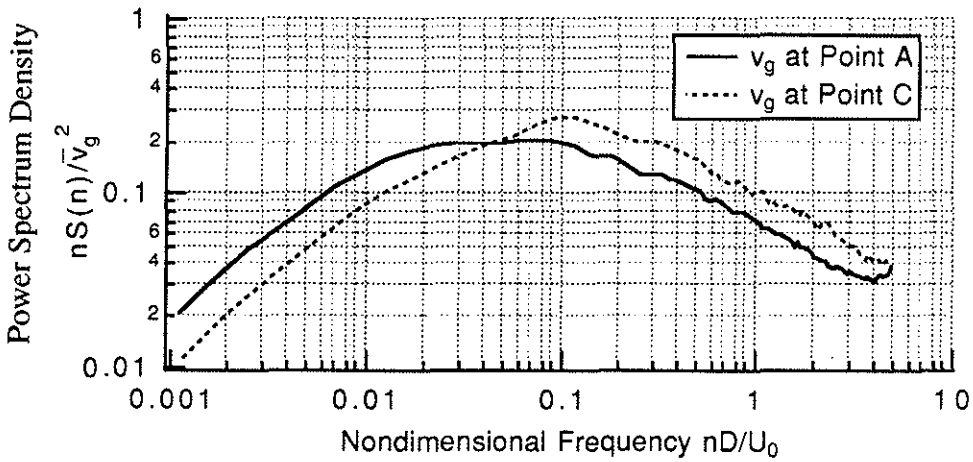

(2) $\mathbf{V}_g$

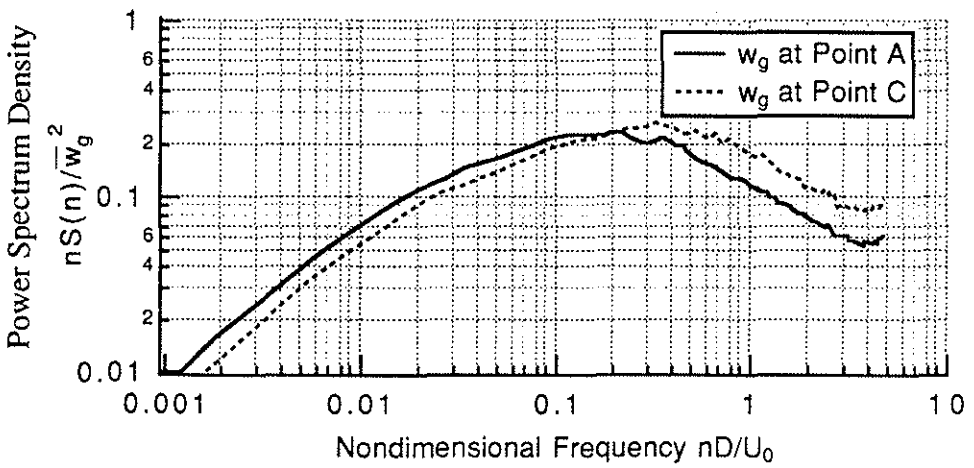

(3) $\mathbf{W}_g$

Figure 5 Power spectral density of measured wind.

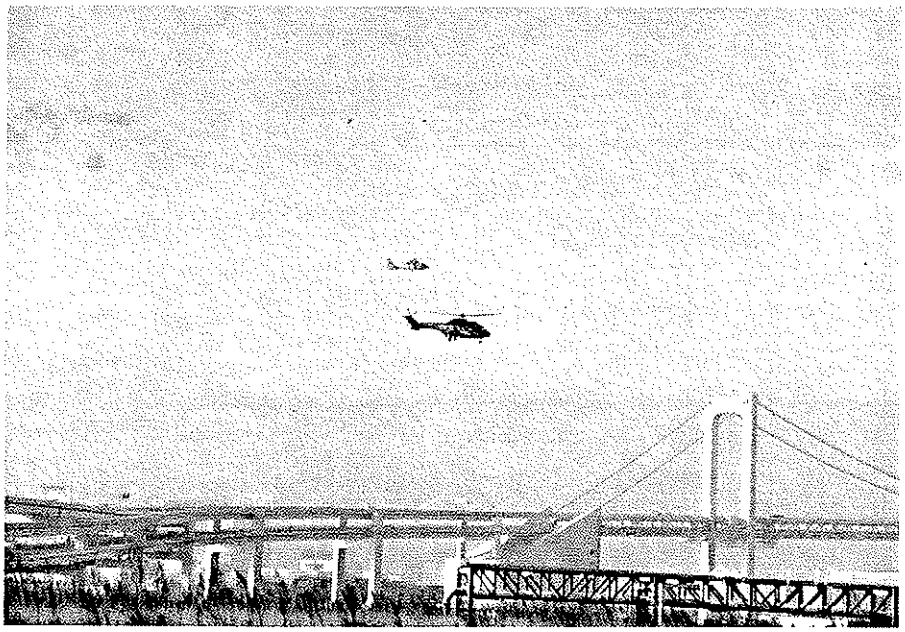

(a) Flight test A.

(b) Flight test B.

Figure 7 Photographs of flight tests.

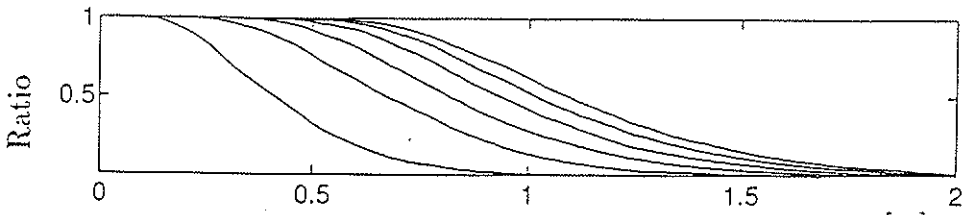

(a) For the circumferential direction.

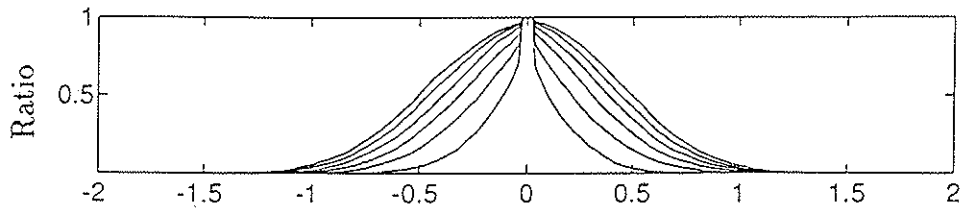

(b) For the longitudinal direction.

Figure 8 Ratio of fluctuation of helicopter position (Point A).

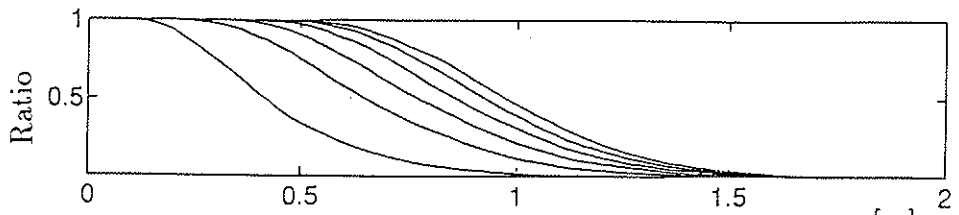

(a) For the circumferential direction.

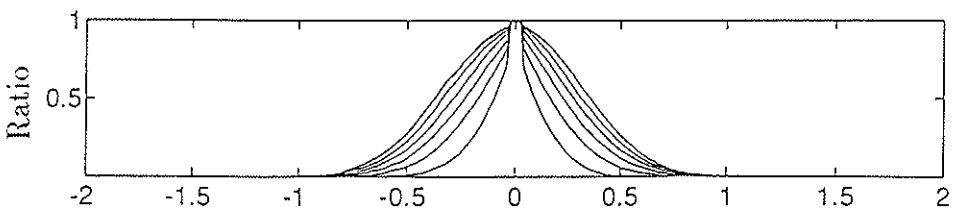

(b) For the longitudinal direction.

Figure 9 Ratio of fluctuation of helicopter position (Point C).

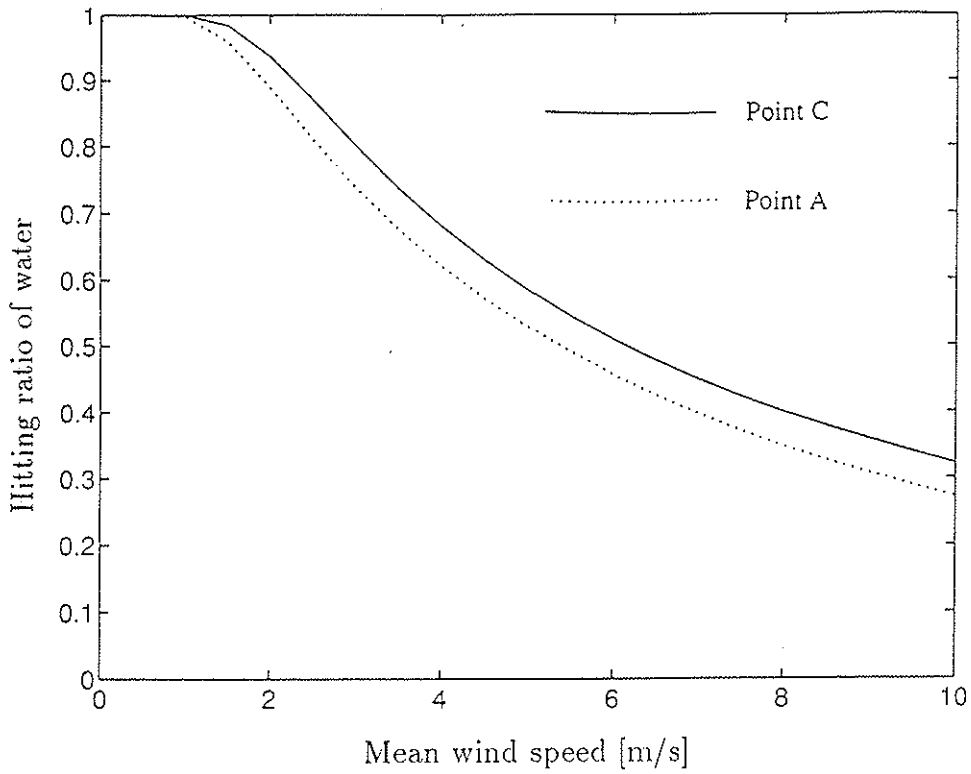

Figure 10 Effect of the hovering point on the hitting ratio.

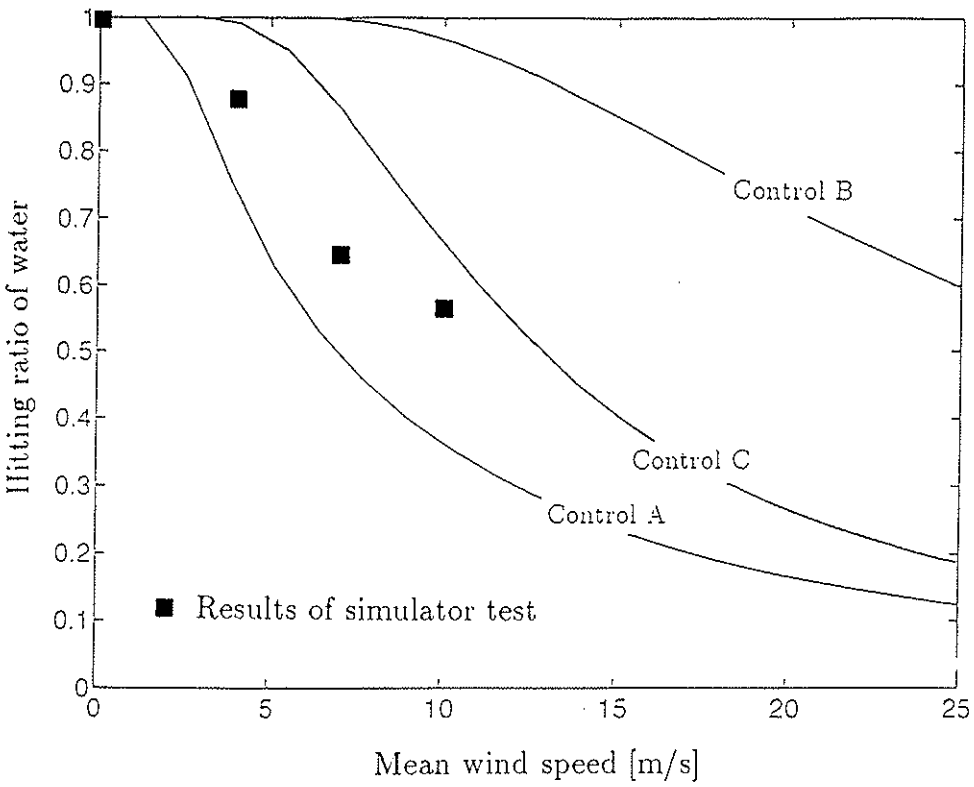

Figure 11 Effect of the control law on the hitting ratio.

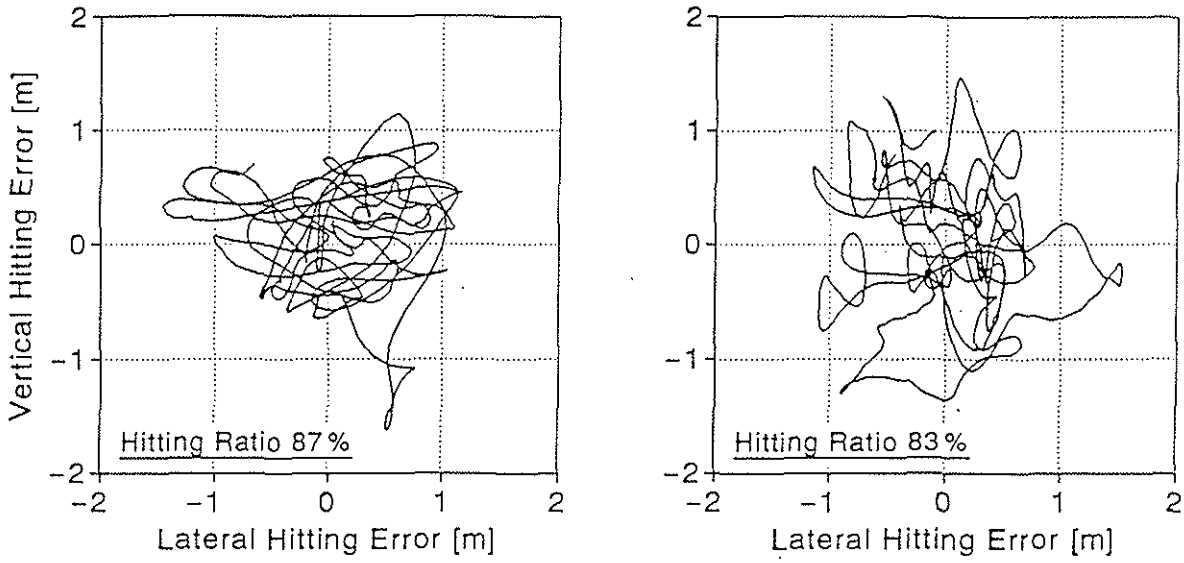

(a) Simulation test.

(b) Flight test B.

Figure 12 The traces of hitting point.

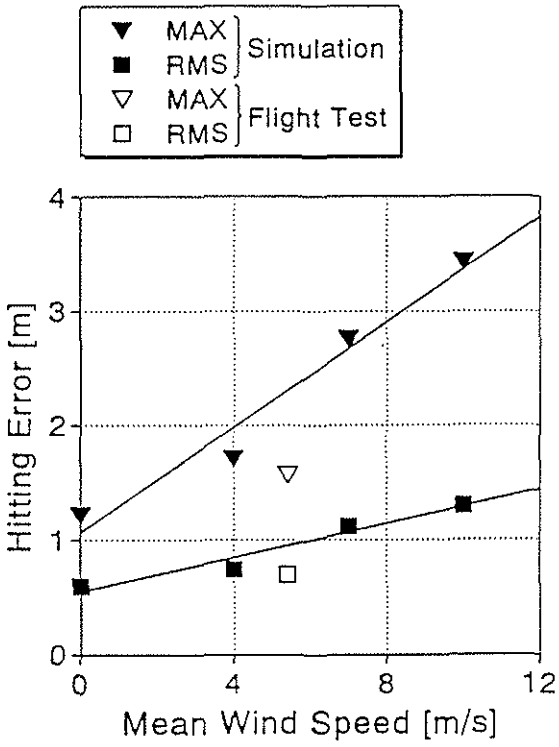

Figure 13 The hitting errors vs. mean wind speed.

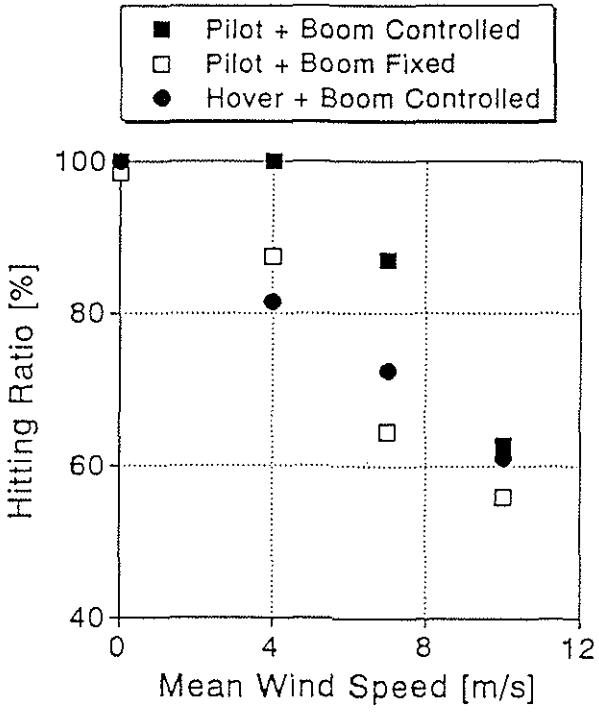

Figure 14 Comparison of the hitting ratio among three tasks.

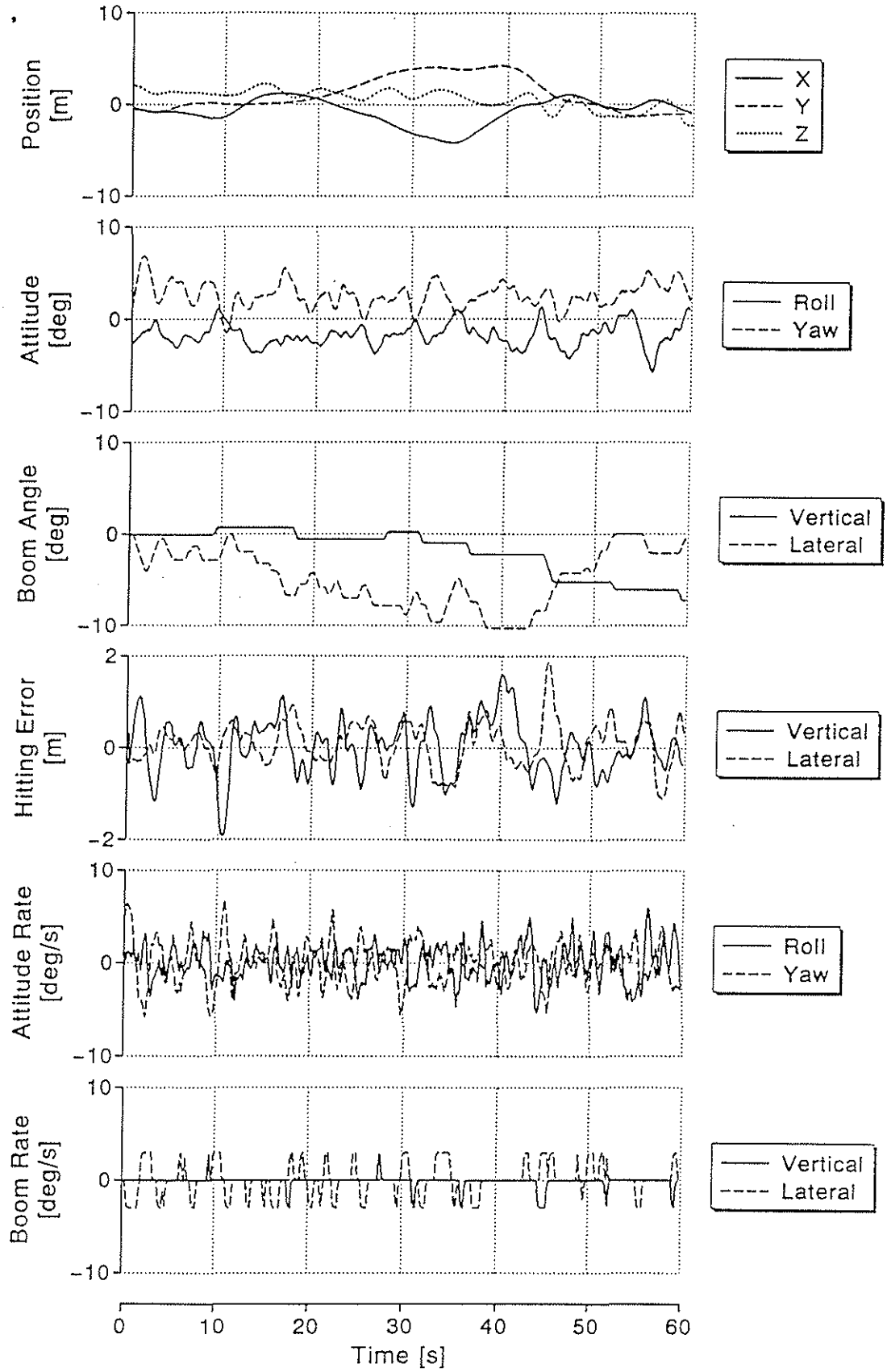

Figure 15 Time histories of the simulated boom operation.

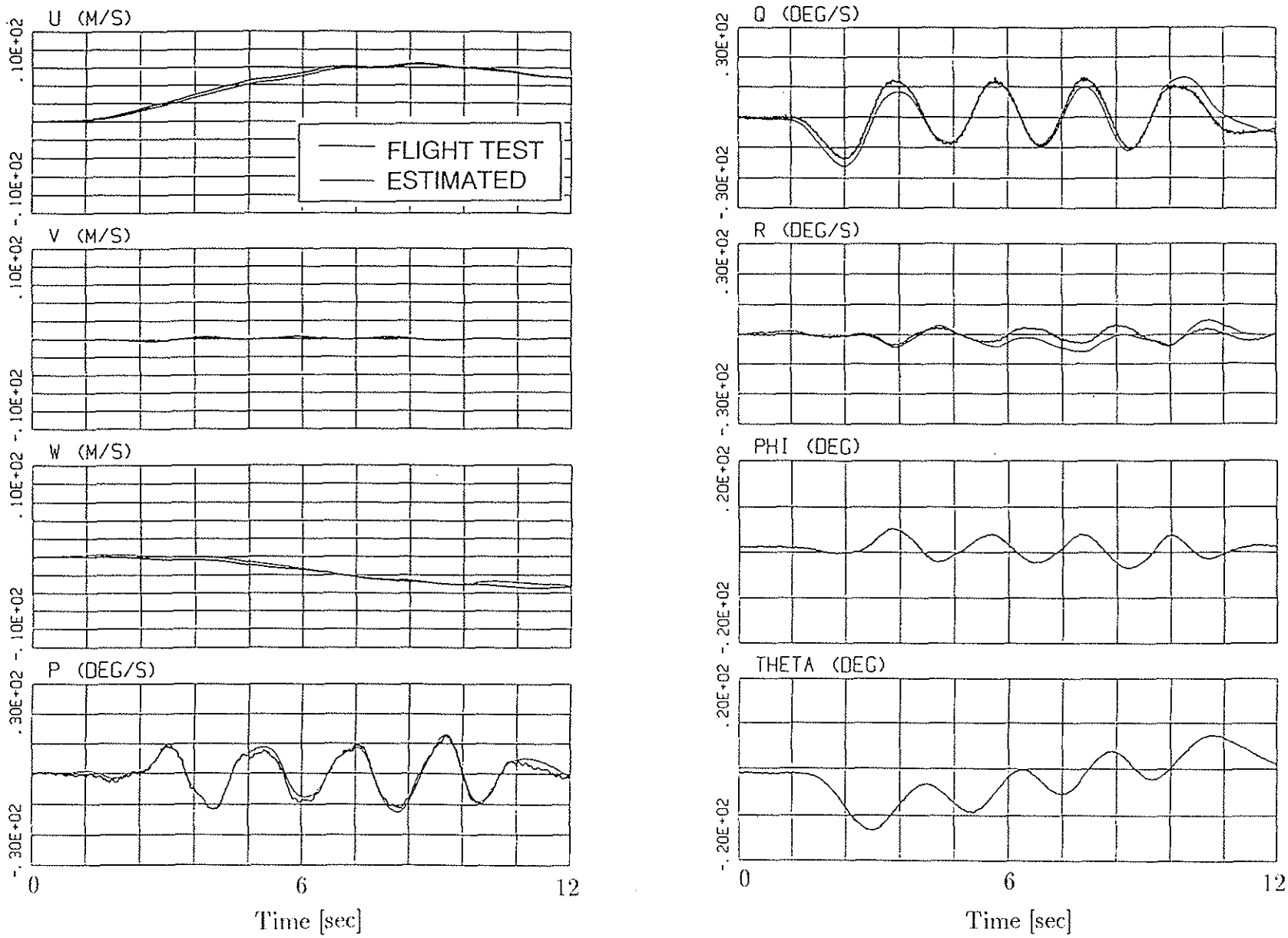

Figure 16 Comparison of the reconstructed and flight test results.

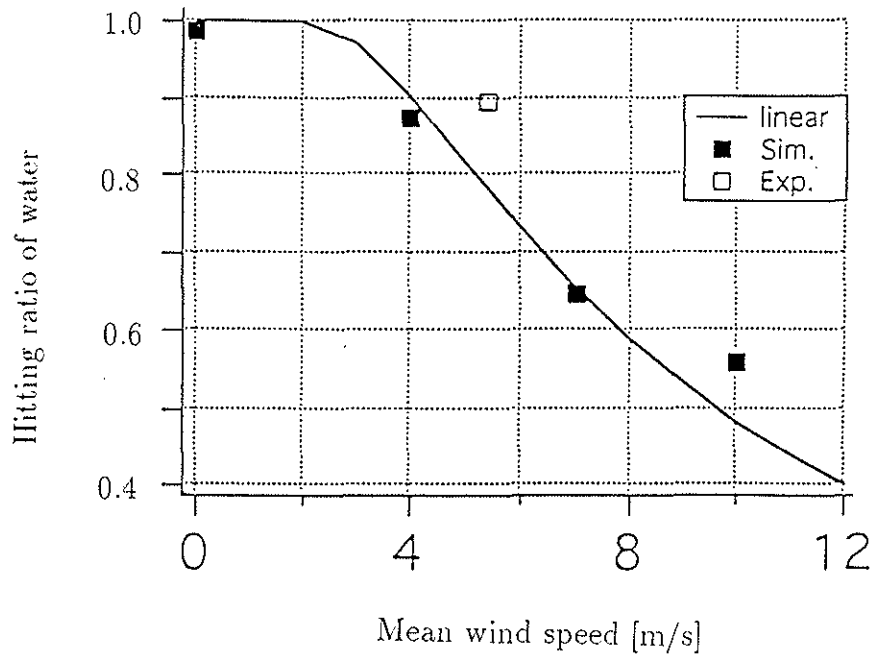

Figure 17 Comparison of the hitting ratio among three methods.

Table 1 The aerodynamic derivatives identified from the flight test A.

A Matrix

A	u	w	q	v	p	r
X	-0.0362	-0.0362	0.0108	0.0235	-0.0822	0.1620
Z	-0.2190	-0.1280	0.5670	-0.0079	-0.8700	-0.1940
M	0.0281	0.0033	-0.1060	-0.0113	0.1520	-0.0785
Y	0.0184	-0.0060	-0.3080	-0.1580	0.6110	0.8590
L	-0.0584	-0.0042	-0.1020	-0.0857	-1.0300	0.4660
N	-0.0174	-0.0084	0.3450	0.0570	-0.4210	-0.6910

B Matrix

B	θ_{0M}	θ_s	θ_c	θ_{0T}
X	1.6600	-8.5700	2.8400	-0.3880
Z	-59.1000	-2.9300	1.9300	-0.9510
M	-1.1700	4.4600	-1.7300	-0.0902
Y	4.9500	0.4930	0.8840	-5.1300
L	3.6400	2.1100	20.1000	-4.0900
N	-9.0400	-0.0215	5.4200	4.6500